Electronic Supplementary Material (ESI) for Lab on a Chip.
This journal is © The Royal Society of Chemistry 2019

A Label-Free Microfluidic Assay to quantitatively study antibiotic diffusion through lipid membranes

J. Cama, C. Chimerel, S. Pagliara, A. Javer and U. F. Keyser

SUPPLEMENTARY INFORMATION

Theoretical Model and Analysis Details

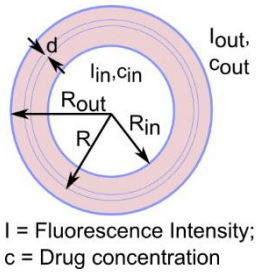

Figure S1. Giant Unilamellar Vesicle schematic.

A giant unilamellar vesicle created by electroformation is shown schematically in Figure S1. A lipid bilayer separates the interior from the exterior of the vesicle. Fluorescence intensities within the vesicle I_{in} are related to the concentration of the drug inside the vesicle c_{in}.

Preliminary confocal measurements on vesicles suspended in a bath of norfloxacin proved that although the concentration of norfloxacin that is diffusing into the vesicles (c_{in}) is dependent on time, its spatial concentration within the vesicle is uniform (Figure S2).

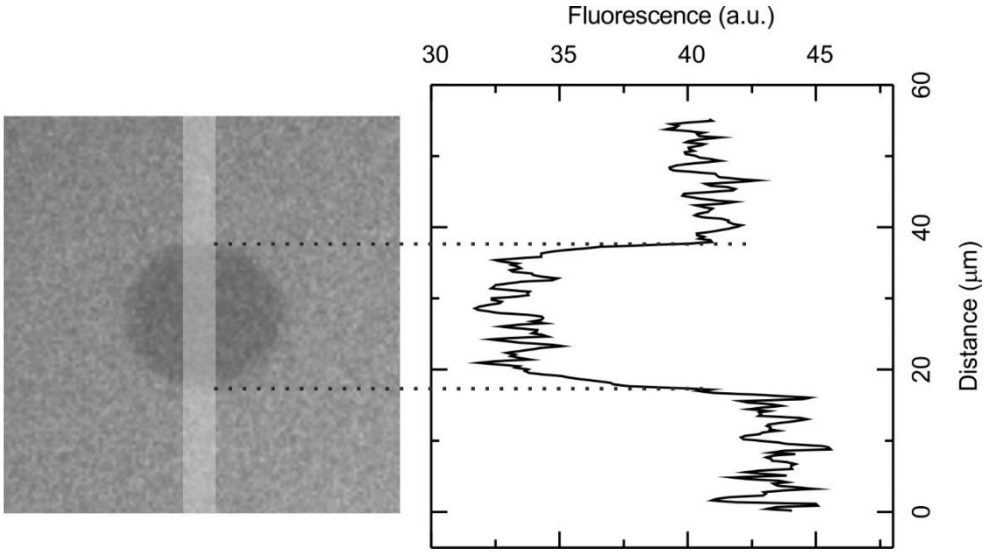

Figure S2. Confocal image (λ_{ex} = 351 nm) of a DPhPC lipid vesicle in a bath of 1.8mM norfloxacin. The flat intensity profile inside the vesicle shows that the distribution of molecules has no spatial dependence within the vesicle. Image from CC PhD thesis.

Thus the rate limiting step in the diffusion process is membrane permeation. The flux of norfloxacin molecules passing through the membrane at a given time t is thus given by:

$$\frac{J(t)}{4\pi R^2} = -KD\frac{dc}{dR} \qquad (1)$$

which on integration gives:

$$J(t) = 4\pi R_{in} R_{out} \frac{KD}{d} (c_{out} - c_{in}(t)) \quad (2)$$

where D is the diffusion coefficient and K the partition coefficient. The drug concentration outside the vesicle c_{out} stays constant over time. Since the thickness (d) of the bilayer (~ 5 nm, Alberts et al, *Molecular Biology of the Cell*) is 3-4 orders of magnitude less than the radius (R) of the vesicles being considered, we may assume that the inner and outer radii are the same, i.e, $R_{in} \sim R_{out} = R$.

The flux of particles passing through the membrane per unit time also equals the variation in the number of particles trapped inside the vesicle. Since within the vesicle the norfloxacin concentration is homogeneous, we can write:

$$J(t) = \frac{dc(t)}{dt} \frac{4\pi R^3}{3} \quad (3)$$

Equating (2) and (3), we get:

$$\frac{dc(t)}{dt} = \frac{3KD}{Rd} (c_{out} - c_{in}(t)) \quad (4)$$

Solving this with boundary conditions:

- $c_{in}(t = 0) = 0$
- $c_{in}(t = t_f) = c_{in}(t_f)$

and defining the Permeability Coefficient $P = KD/d$, we obtain the solution:

$$ln\left(\frac{c_{out} - c_{in}(t)}{c_{out}}\right) = -3\frac{Pt}{R} \quad (5)$$

The drug concentration outside the vesicle is directly proportional to the fluorescence intensity I_{out}. However, since the optical setup used in the microfluidics experiments is not a confocal microscope, the drug concentration inside the vesicle ($c_{in}(t)$) depends on the fluorescence intensity inside the vesicle I_{in} in a more complicated manner. We can split the intensity contribution inside the vesicle into two parts, one that is the contribution of the drug ($I^{true}_{in}(t)$) and another that is simply due to the out of focus light from outside the vesicle that has entered into the region being studied, that we label F. F is independent of time (since it is independent of drug concentration) but has a dependence on the vesicle radius. Now,

$$\frac{c_{out} - c_{in}(t)}{c_{out}} = \frac{I_{out} - I_{in}^{true}(t)}{I_{out}}$$

We detect vesicles at an initial point that we define as $t = 0$ and at a later time point $t = t_f$. Vesicle detection is performed in a two-step process during image processing. Firstly, deviations from the mean image intensity are detected, and if the difference from the baseline is more than thrice the median absolute deviation (MAD), the frames are considered for potential vesicle detections. Secondly, the vesicles are identified in each of the candidate regions. A background is calculated as the averages of the frames just before and after each detection event. This background is then subtracted from each of the images in the candidate region in order to enhance the vesicles, as they are the main source of intensity variation. A binary mask with the vesicle outline is obtained using the threshold given by the Otsu method. Finally, the 'regionprops' function in MATLAB is used to obtain information about the major and minor axes, the centre of the shape, amongst other parameters. The vesicle radius is determined by taking an average of the semi-major and semi-minor axes. Since we capture the vesicles for multiple frames, we can track the movement of the centre position and use this to determine the vesicle velocity. Around the centre, a 5×5 pixel box is created and the average intensity within this box is determined. The average intensity of exactly the same 5×5 pixel box is determined in the background image for each event (the MATLAB analysis codes are attached for examination). This gives us the values of I_{in} and I_{out}, which are used in the calculations.

For clarity, let us define all intensities related to the interior of vesicles at time $t = 0$ as I_1 and at later times t_f as I_2. We reiterate that the intensities outside the vesicles I_{out} remain constant with time, and will always be written as I_{out}. Our image analysis program outputs the following value for each vesicle at the two time points:

$$\Delta I_1 = \frac{I_{out} - I_1}{I_{out}} \quad (t = 0)$$

$$\Delta I_2 = \frac{I_{out} - I_2}{I_{out}} \quad (t = t_f)$$

Now,

$$I_1 = I_1^{true} + F = F$$

since we assume that the drug concentration inside the vesicle is 0 at $t = 0$. Furthermore,

$$I_2 = I_2^{true} + F = I_2^{true} + I_1$$

Therefore,

$$I_2^{true} = I_2 - I_1 = I_{in}^{true}(t)$$

Thus,

$$\frac{c_{out} - c_{in}(t)}{c_{out}} = \frac{I_{out} - I_{in}^{true}(t)}{I_{out}} = \frac{I_{out} - (I_2 - I_1)}{I_{out}} = \Delta I_2 + \frac{I_1}{I_{out}} = \Delta I_2 + 1 - \Delta I_1$$

Substituting this expression in (5), we finally obtain our working equation:

$$ln(\Delta I_2 - \Delta I_1 + 1) = -3\frac{Pt}{R} \quad (6)$$

Note that it is the contribution of F in I_1 that causes the radial dependence of ΔI in the $t = 0$ (black) points in Figure 2 of the main text, and in Figure S4 below. The radial dependence of ΔI at later time points (red circles) is both due to F as well as due to the radial dependence of drug diffusion.

Rearranging the above equations, we can also write:

$$\frac{I_2}{I_{out}} = 1 + \frac{I_1}{I_{out}} - e^{-\frac{3Pt}{R}} \quad (7)$$

We use this exponential dependence to determine P from Figure 3a in the text. Since we measure the dependence on length (L) travelled in the chip, we can rewrite the above equation using the values of the average velocity and radius. Further, since we defined $I_1 = I_{in}(L=0, t=0) = F$ and $I_2 = I_{in}(L=L, t=t_f)$, we can write:

$$\frac{I_{in}(L)}{I_{out}(L)} = 1 + \frac{I_{in}(0)}{I_{out}(0)} - e^{-\frac{3PL}{v_{avg} \cdot R_{avg}}} \quad (8)$$

Though $I_{out}(L) \sim I_{out}(0)$, they have been written out explicitly since we measured the background intensities at both points.

Since we detect each vesicle for multiple frames as it passes through the field of view, we can determine its average velocity from a knowledge of the centre positions and frame rate. We use this to determine the time taken for the vesicle to travel from the first detection region (Length = 0, $t = 0$) to the final detection region (Length = L, $t = t_f$). We also determine the average value of ΔI across the entire detection event, the average radius and the average value of I_{in}/I_{out}. To ensure that only suitably circular vesicles are analysed, we determine the ratio of the minor axis to the major axis for each vesicle and only select those events for which this ratio is 0.75 and above. A few vesicles with diameters larger than the channel width were detected (these were deformed as they squeezed into the channel). These were discarded from the analysis as we believed they might be susceptible to rupture and leakage. It was also decided to discard detections of vesicles under 18 pixels (256 pixels = 120 μm in our images) in radius since on inspection of the images it was found that these were occasionally pieces of lipid junk rather than vesicles. Our program saves the raw images of vesicle detection events making it possible to check the raw vesicle images manually as well.

Finally, we must determine the value ($\Delta I_2 - \Delta I_1 + 1$) for vesicles of the same radius. From the data, it is clear that in the absence of the drug inside the vesicle (i.e, at $t = 0$), the normalised intensity contributions measured (ΔI_1) depend linearly on vesicle radius. We fit this to a linear equation and use this fit to find the equivalent values of ΔI_1 for each vesicle radius detected at a later time. Thus for each value of ΔI_2 and the corresponding detected radius R, we determine ΔI_1 and use this in our calculations.

As a minor note, in determining ΔI_1 and ΔI_2, we divide by ($I_{out} - 505$) rather than I_{out}, since 505 (a.u) is the dark noise associated with the camera in the absence of any illumination. The value 505 is much lower than the typical intensities detected (>15,000) and is a minor correction. Similarly, in Figure 3a in the main text, I_{in}/I_{out} actually equals ($I_{in} - 505$)/($I_{out} - 505$). The difference is negligible and does not affect the result.

It must be mentioned here that three outliers were removed from Figure 3b in the main text, since we believe that the vesicles in question were leaky and hence significantly off the line. This represents about 1% of the total number of events.

The Permeability coefficients measured are independent of vesicle velocities

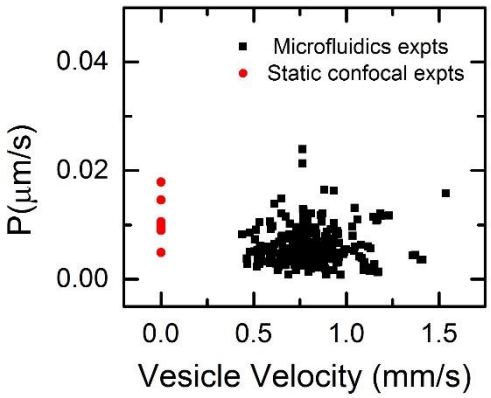

Figure S3. Plot of Permeability Coefficient (P) as a function of Vesicle Velocity. No significant dependence is seen, indicating that hydrodynamic effects do not significantly influence the permeation of norfloxacin in our microfluidic environment at the relevant flow velocities.

To study any potential effect of hydrodynamics or vesicle shear on the determination of the permeability coefficient (P), we have plotted the values of P obtained (pH 7) for individual vesicles against the corresponding vesicle velocities in Figure S3 above. We have included the preliminary measurements performed on stationary vesicles (N=7) in a confocal microscope (λ_{ex} = 351 nm, red circles in Figure S3). It is clear from the plot that there is no influence of vesicle velocity on the permeability coefficient at the relevant flow velocities. If there were indeed an influence of hydrodynamics on drug permeation, one would have expected to see a dependence of P on the vesicle velocity. We therefore believe our technique and analysis to be robust in the microfluidic regime. We reiterate here that we define a strict circularity condition to ensure that we perform the permeability analysis only on vesicles that are suitably circular, and thus reject vesicles that are damaged by shear. Besides the circularity condition, vesicles of diameters larger than the channel width are rejected before analysis, since these are more susceptible to shear and rupture due to contact with the channel walls. Furthermore, we are also capable of checking the vesicles manually by viewing the raw images of vesicle detection events. These are used to reject the few 'bad events' that evaded our strict applicability criteria.

Complete Data Set

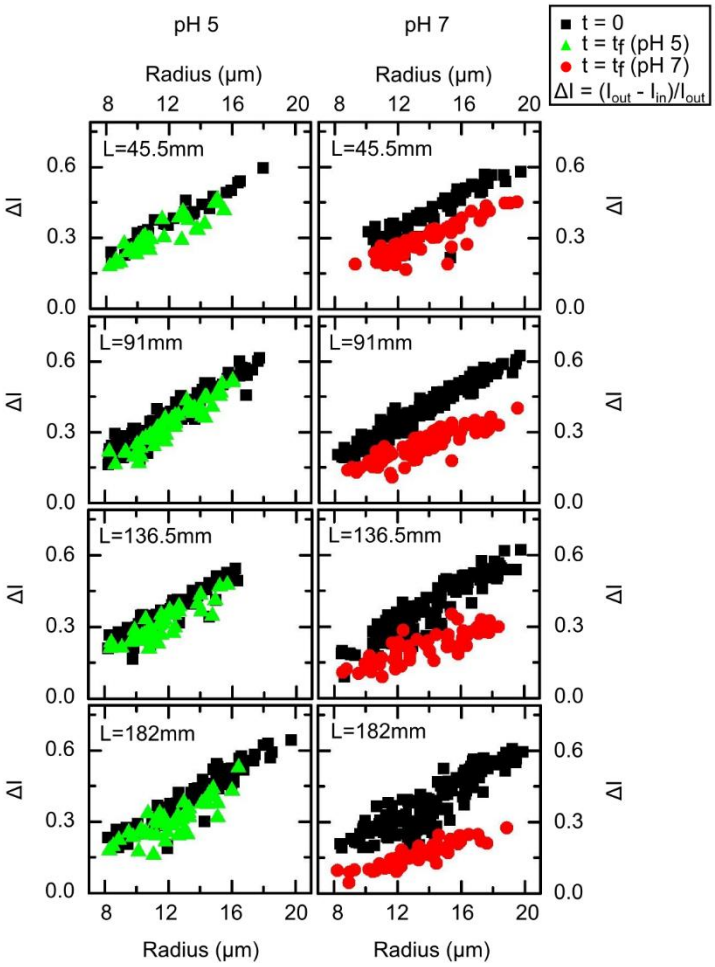

Figure S4. Plots of ΔI vs R for all positions measured, at pH 5 (left) and pH 7 (right). As the length (L) travelled by the vesicles increases, I_{in} increases significantly at pH 7 and correspondingly ΔI decreases. Thus as L increases, the difference between the t = 0 (black squares) and t = t_f (red circles) becomes correspondingly larger. This effect is much smaller at pH 5, where the black (t = 0) and green (t = t_f) points overlap significantly. This suggests that the drug is diffusing across the lipid membrane much faster at pH 7 than at pH 5. The radial dependence of ΔI is due to the dependence of F (the out of focus light contribution) on radius for the black points (t = 0), and due to both F and the drug diffusion for the red points (t = t_f), as mentioned in the analysis above.

Description of AVI file

The AVI file attached in the electronic supplementary materials is the combination of a series of image acquisitions taken in an experiment (at pH 7) where the length from the $t = 0$ to the $t = t_f$ detection point was 136.5 mm (i.e, $L = 136.5$ mm). The AVI file was constructed by combining (in ImageJ) a typical selection from the tiff stacks acquired in an experiment, without any compression (AVI frame rate = 20 fps). A number of vesicle detection events in the two regions of interest are observed. In the channel on the left ($t = 0$), the vesicles are darker than the vesicles that appear in the channel on the right ($t = t_f$), indicating that I_{in} increased as the vesicles progressed along the network. The autofluorescence background in the two channels is the same, showing that I_{out} is constant as required in the detection regions. Furthermore, it is clear that each of the vesicles is detected for a number of frames, allowing an accurate measurement of parameters such as radius and internal fluorescence intensities for individual vesicles.

Norfloxacin Fluorescence Calibration

To determine the minimum concentration of norfloxacin that could be detected by our camera, we performed a calibration by pipetting droplets of different norfloxacin concentrations (prepared in the pH 7 buffer used in experiments) in between two glass coverslips. The droplets were suspended between the two coverslips as measuring the intensity in a droplet simply placed on a single coverslip is susceptible to variation due to the curvature of the droplet. The EM gain was set at 20, to ensure that the intensity histogram peaks were in the middle of the camera range (correspondingly, the EM gain in the actual experiments was set to 100 since in the PDMS chip, this gave the fluorescence histogram peaks in the centre of the range. This is due to the fact that the light scatters differently in PDMS and glass). The minimum concentration of norfloxacin that could be detected using its autofluorescence at an excitation wavelength of 340 nm was found to be around 50 μM.

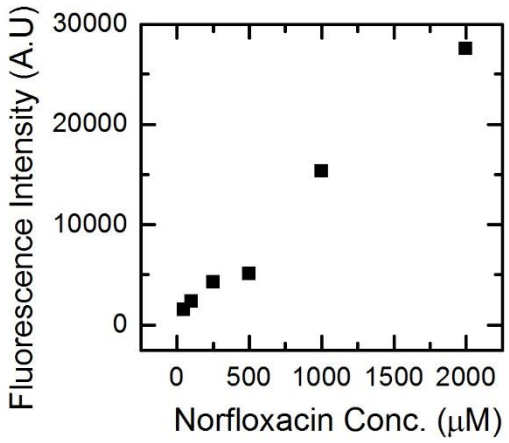

Figure S5. Fluorescence intensity profile of norfloxacin at 340 nm excitation. Camera EM gain 20, 2ms exposure, bin 2, clearing pre-sequence.